

Present-day kinematic pattern of the Northern - Central Italy from GPS measurements

Cenni N.^(a), Baldi P.^(b), Mantovani E.^(a), Viti M.^(a), Babbucci D.^(a), Tamburelli C.^(a) and Bacchetti M.^(b)

(a) Dipartimento di Scienze della Terra - Università degli Studi di Siena. (b) Dipartimento di Fisica - Università degli Studi di Bologna.



Introduction

The post-early Pleistocene deformation recognized in the Central Mediterranean region may plausibly and coherently be explained as an effect of the convergence of the confining plates, as argued by Mantovani et al. (2009a) and Viti et al. (2011). In response to the motion of Africa and the Anatolian-Aegean system with respect to Eurasia, the Adriatic plate (Adria) has moved as indicated in figure 1. This plate kinematics has considerably influenced the tectonics of the Apennine belt, since the outer sector of this chain, constituted by the Molise-Sannio (MS) units, the eastern part of the Lazio-Abruzzi carbonate platform (ELA), the Romagna-Marche-Umbria (RMU) and the Toscana-Emilia (TE) units, being stressed by the Adriatic plate, has undergone a roughly NE to North ward extrusion (Fig. 2). The outward migration of the escaping wedges has caused extensional deformation along their inner margin and compressional deformation along the outer fronts (Fig. 2). Considering the offsets of the thrust faults generated in the Pliocene evolutionary phase and cut by younger normal faults, as evidenced by the seismogeological section CROP-03 (Finetti et al., 2005), one can tentatively estimate the average long term migration rate of the RMU wedge during the Quaternary. This analysis suggests a velocity of 3-5 mm/yr (Mantovani et al., 2009b). Vertical movements in the study area are mostly characterized by uplift of orogenic zones and subsidence of basins. The uplift pattern in the Alps suggests that the indentation of the Adriatic plate is the main driving mechanism. The general uplift observed in the Apennines, with moderate rates, may be an effect of the longitudinal shortening of this belt. The Po basin is characterized by the Pliocene-Quaternary sedimentary sequence which is up to 8 km thick along the southern edge of the Plain, at the morphological boundary with the Apennines. Active thrusts, related to tectonics in the Apennines, are buried beneath the Quaternary sediments of the eastern Po Plain.

By considering stratigraphic data provided by industrial wells, the long term subsidence rate due to ground settlement in the Po valley has been estimated in about 1 mm/yr.

The main cause of subsidence in the Po plain area is related to anthropogenic activities. In the second half of the 20th century, the increase in economic activities in the region and the consequent pumping water and gas from underground reservoirs, induced subsidence with rates up to 70-100 mm/yr in the Po Delta and near the Bologna city. In recent times, after a strict regulation of this phenomenon, subsidence rates have considerably decreased, now ranging between few mm/yr and about 10 mm/yr, with highest velocities along the eastern padanian margin of the Apennines (Fig. 6). Minimum values of subsidence rate coincide with a relatively low thickness of Pliocene and Quaternary sediments at the top of the buried thrust-related anticlines.

The dense network of GPS permanent stations allows a fairly accurate monitoring of the present kinematic pattern in the study area.

Horizontal kinematic pattern

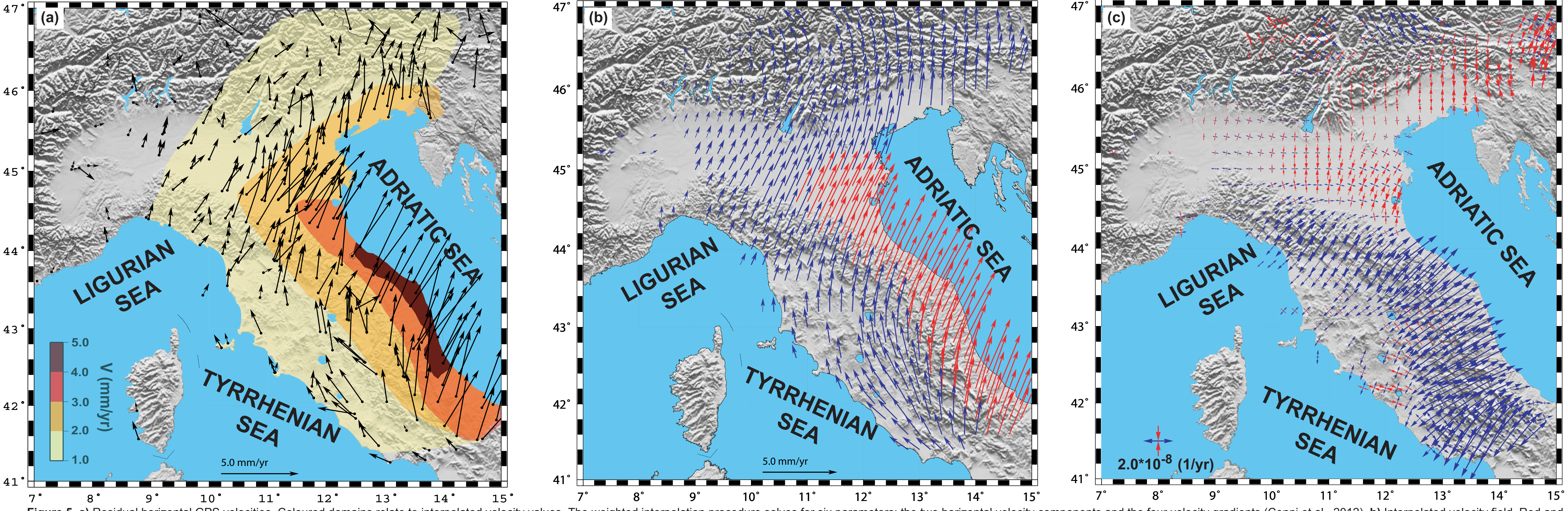


Figure 5. a) Residual horizontal GPS velocities. Coloured domains relate to interpolated velocity values. The weighted interpolation procedure solves for six parameters: the two horizontal velocity components and the four velocity gradients (Cenni et al., 2012). b) Interpolated velocity field. Red and blue arrows respectively indicate rates greater and lower than 2.5 mm/yr. c) Strain field related to the interpolated velocity field. Red converging and blue diverging arrows indicate principal axes of shortening and lengthening respectively.

The observed ITRF2005 residual horizontal velocity pattern with respect to an Eurasian frame is shown in figure 5a. The interpolated velocity field and the related horizontal strain rate pattern are illustrated in Figs. 5b and 5c. The velocity field indicates that a long sector of the outer part of the belt, comprising the RMU wedge and the eastern part of the TE wedge, moves significantly faster (3-4 mm/yr) and more easterly with respect to the surrounding zones, where velocities are mostly lower than 2 mm/yr. This evidence is fairly significant, being coherently indicated by many velocity vectors. One may note that the faster domain roughly corresponds to the Apennine sector that has been characterized by greater mobility since the middle Pleistocene (Figs. 1 and 2). This similarity might suggest that the dynamic context that acted in the most recent tectonic evolution, causing the lateral escape of the RMU wedge, is still going on and that, consequently, such extrusion may be almost continuous over time (Cenni et al., 2012). The strain rate field (Fig. 5c) points out fairly coherent regimes in the various sectors of the zone considered. A compressional regime, with SSE-NNW shortening axis, dominates in the Eastern Alps, at the northern collisional border of the Adriatic plate with the Eurasian domain. A roughly N-S compression, associated with minor orthogonal lengthening, affects the padanian zone facing the most mobile sector of the belt. A dominant extensional regime, with SW-NE lengthening axis coherently occurs in the main Northern Apennine chain. A transient regime mainly occurs in the Central Apennines.

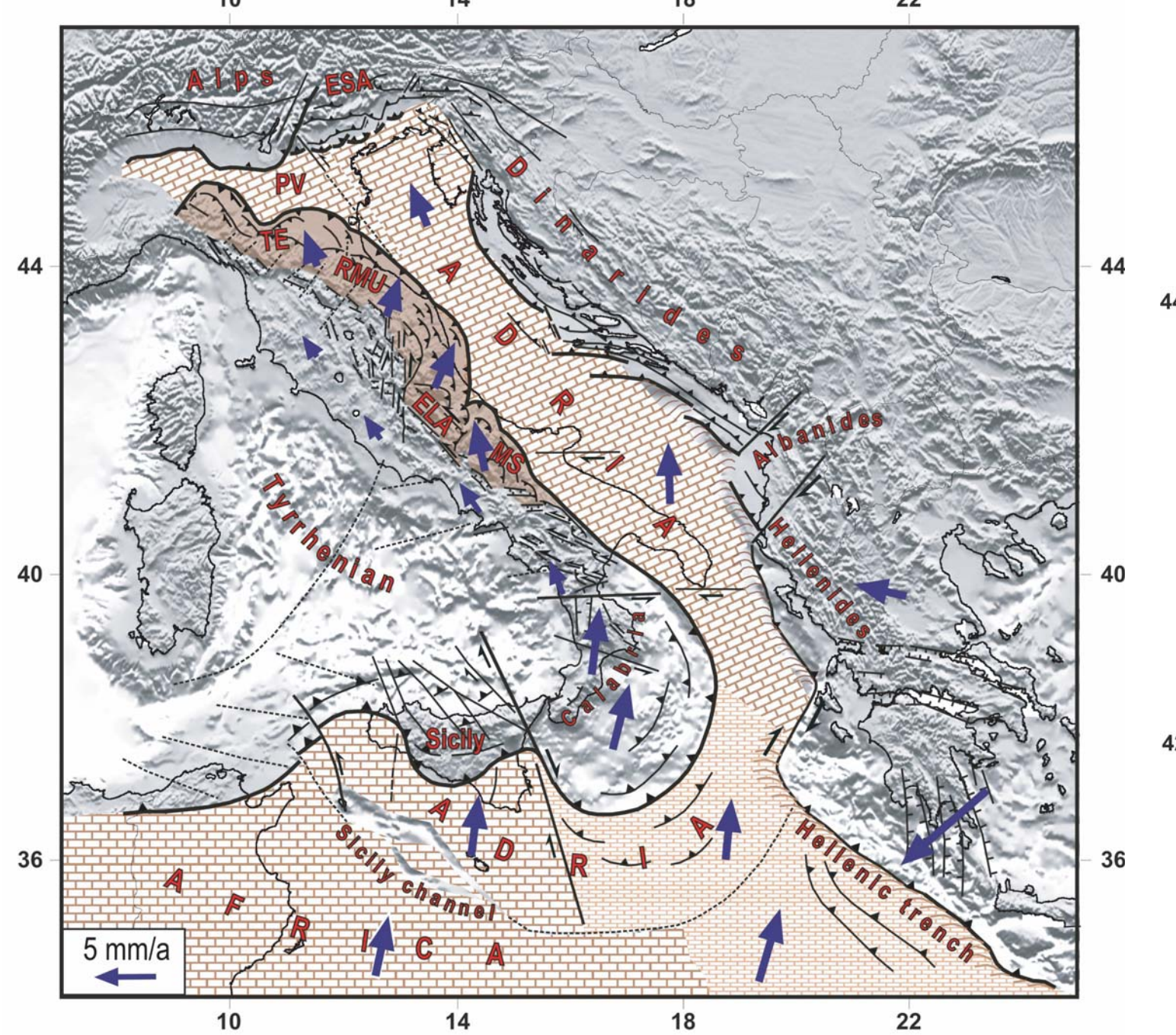


Figure 1. Tectonic setting and kinematics in the Central Mediterranean area, compatible with the post-early Pleistocene deformation pattern (Viti et al., 2011; Mantovani et al., 2009a,b): 1-2) African and Adriatic continental domains; 3) oceanic Ionian domain 4) outer sector of the Apennine belt carried by Adriatic plate (Adria) 5,6,7) main compressional, extensional and transcurrent tectonic lineaments. Blue arrows indicate the long-term kinematic pattern (middle Pleistocene to Present) with respect to Eurasia. ELA = Eastern Lazio-Abruzzi platform, EA = Eastern Southern Alps, MS, RMU, TE = Molise Sannio, Romagna-Marche-Umbria and Toscana Emilia tectonic wedges, PV = Po valley.

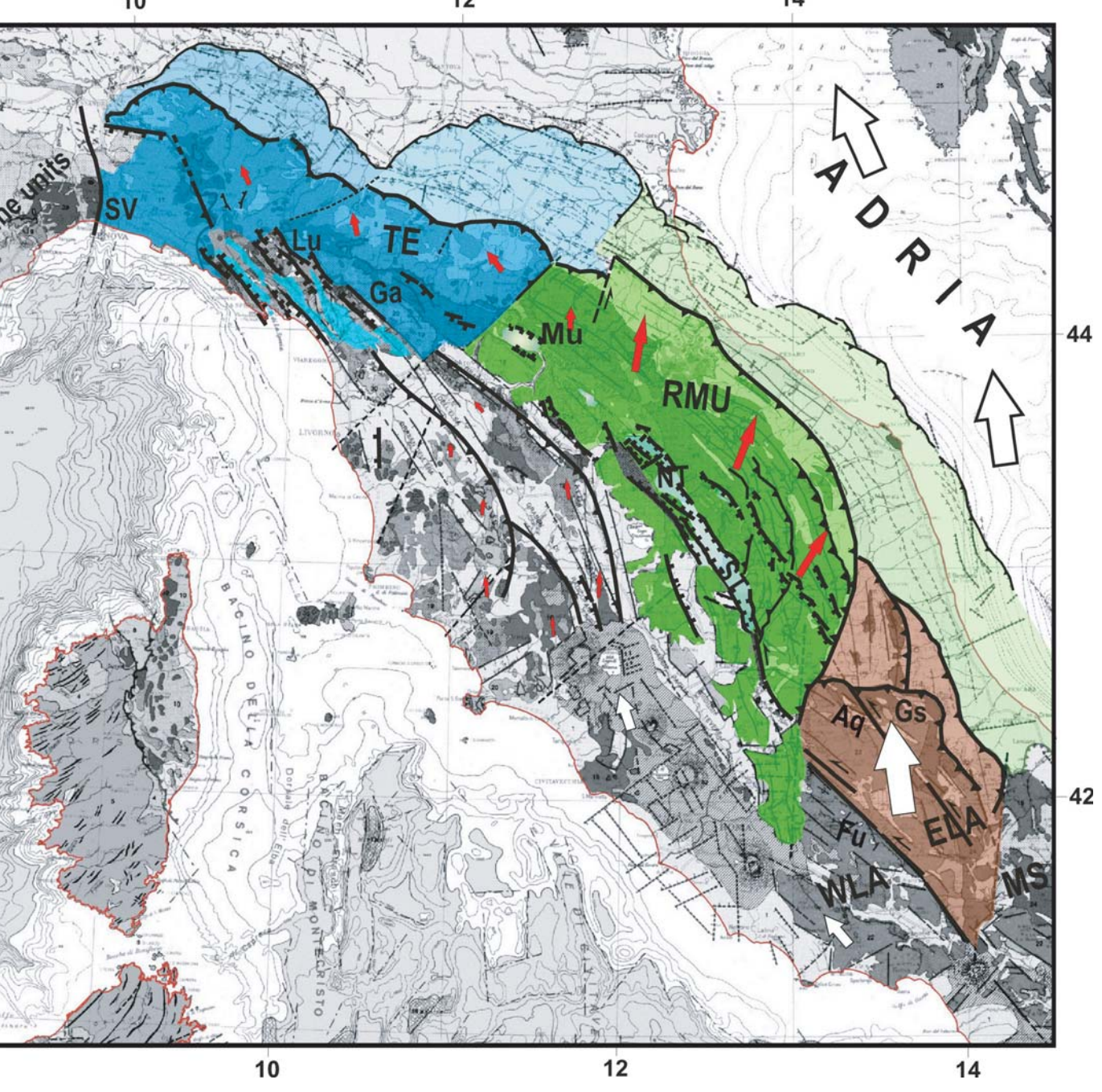


Figure 2. Post early Pleistocene tectonic setting in the study area, reported on the Carta Tettonica d'Italia (Funicello et al., 1981). The longitudinal shortening of the Northern Apennines, driven by the push of the eastern Lazio-Abruzzi platform (ELA), is accommodated by the lateral escape of the Romagna-Marche-Umbria (RMU) and Toscana-Emilia (TE) wedges in the framework of the large scale geodynamics sketched in figure 1. White and red arrows indicate the kinematics of Adria, ELA and Northern Apennines respectively. Aq, Fu=Aquila and Fucino transensional fault systems, Ga=Garfagnana trough, GS= Gran Sasso arc, Lu= Lunigiana trough, MS = Molise-Sannio wedge, Mu=Mugello trough, NT=Northern Tiber trough, ST=Southern Tiber trough, SV= Sestri-Voltaggio lineament, WLA= Western Lazio-Abruzzi platform. Symbols as in figure 1.

Vertical velocity field

The kinematic pattern given in Fig. 6 indicates that the sites located in the Alpine and Apennine belts are mostly characterized by uplift, while three areas are affected by subsidence: the Po Plain, the western sector of the Arno Plain and some Central Apennine basins. In the Alps, uplift rates are of the order of a few mm/yr, in agreement with previous estimates carried out by repeated levelings in the last century. At present, the uplift of that zone is attributed to the combined effects of tectonic shortening, postglacial isostatic rebound, flexural response to climate-driven denudation and rapid glacier shrinkage. The observed uplift in the Northern Apennines, mostly lower than 2 mm/yr, is mainly imputable to longitudinal shortening (Mantovani et al., 2009a,b; Cenni et al., 2012). The repeated leveling surveys executed by the Istituto Geografico Militare Italiano (IGMI) over 129 years, along the lines across the chain from the Tyrrhenian to the Adriatic side of the peninsula, provided maximum uplift rates in the range 1-3 mm/yr, with the assumption that most of the Tyrrhenian side of the Central-Northern Apennines is essentially stable. The comparison between the subsiding rates measured at GPS sites in the Po Plain area (Fig. 6) and the results previously obtained by different techniques (1999-2005), such as leveling campaigns and DInSAR analysis (2002-2006), shows that rates are stable or somewhere decreasing in response to drastic reductions of water withdrawal and/or climatic effects. A detailed analysis of the continuous GPS series allows the recognition of space and time variations of subsidence velocities. For example, the rates observed in the MO01 and MODE stations located respectively north and south of Modena city show important variations (Fig. 7), whereas the rates of Ravenna and San Giovanni in Persiceto sites do not show any significant perturbation.

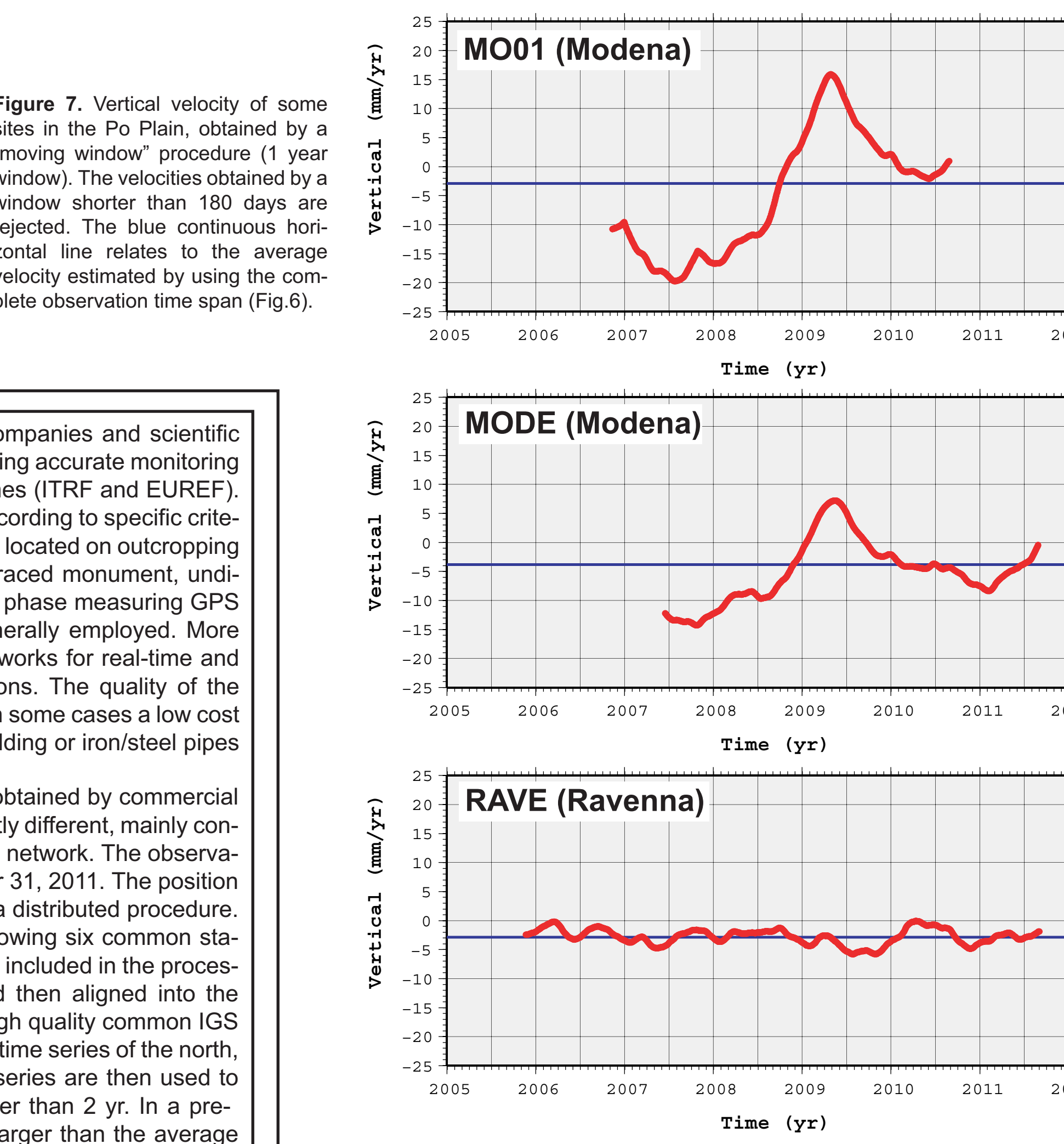


Figure 7. Vertical velocity of some sites in the Po Plain, obtained by a "moving window" procedure (1 year window). The velocities obtained by a window shorter than 180 days are rejected. The blue continuous horizontal line relates to the average velocity estimated by using the complete observation time span (Fig. 6).

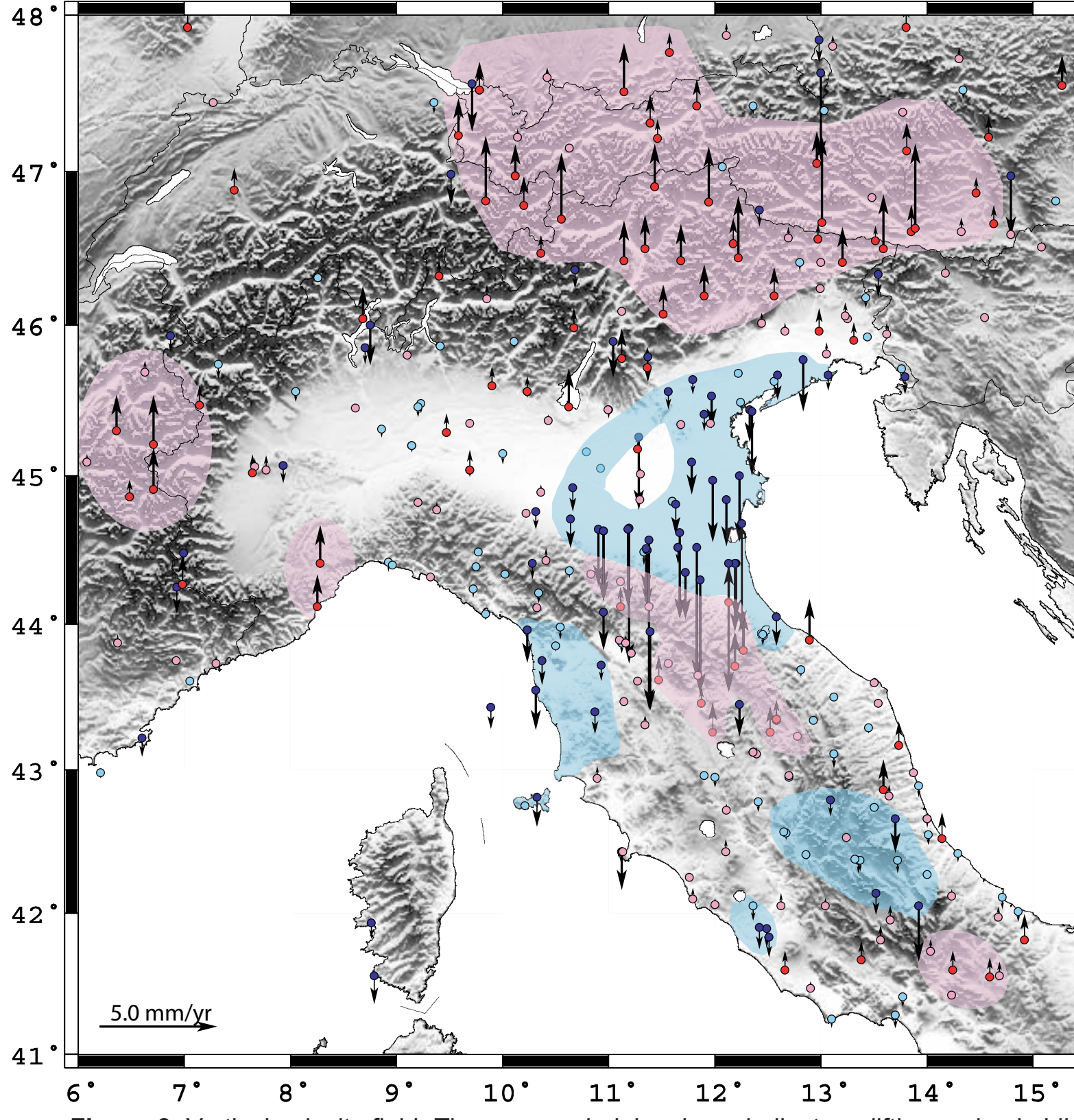


Figure 6. Vertical velocity field. The cyan and pink colours indicate uplifting and subsiding regions respectively.

GPS data analysis



Figure 3. Locations of 289 permanent GPS stations used in this work. Circles and triangles respectively indicate scientific and commercial permanent stations, given in the legend. The inset shows the 6 IGS stations we have used to align the above regional network to the ITRF2005 reference frame.

Many of the stations used in this study (Fig. 3) are managed by public companies and scientific research institutions (Baldi et al., 2009; Cenni et al., 2012), aimed at performing accurate monitoring of earth surface movements and densifying the international reference frames (ITRF and EUREF). Generally, the location and monumentation of these sites are determined according to specific criteria in order to obtain the maximum stability and accuracy, i.e. concrete pillars located on outcropping bedrock or a building with fairly deep foundations, deeply anchored drill-braced monument, undisturbed view of the sky for clear signal reception. Dual-frequency code and phase measuring GPS receivers and IGS standard Dorne Margolin choke ring antennas are generally employed. More recently, some private and public agencies have developed local GPS networks for real-time and post-process positioning services, with a quite dense distribution of stations. The quality of the adopted instruments is usually comparable to that of scientific stations, but in some cases a low cost monumentation procedure (usually a steel bar anchored to the roof of a building or iron/steel pipes solidly connected to supporting walls) is adopted.

This last feature could imply a lower accuracy of data, but a comparison of the results obtained by commercial and scientific stations (Baldi et al., 2009, 2011) indicates that data quality is not significantly different, mainly concerning the noise of the time series. This check has allowed us to densify the available GPS network. The observation periods of the network sites are comprised between January 1, 2001 and December 31, 2011. The position of each GPS has been estimated with the scientific GAMIT/GLOBK software, adopting a distributed procedure. The network is divided into 20 sub-networks (clusters), each including at least the following six common stations: BRAS, CAGL, GRAZ, MATE, WTZR and ZIMM. The IGS precise ephemerides are included in the processing. The daily solutions of the 20 clusters are combined into a unique solution and then aligned into the ITRF2005 reference frame, using the ITRF2005 coordinates and velocities of the five high quality common IGS stations (CAGL, GRAZ, MATE, WTZR and ZIMM). At the end of this procedure, the daily time series of the north, east and vertical components of each site are obtained. These series are then used to assess the three geometrical components of velocity for the sites with an observation period longer than 2 yr. In a pre-processing phase, the data whose deviation from the mean linear trend is three time larger than the average RMS of the position time-series residuals (outliers) have been identified and removed. The daily position component $y_k(t)$, ($k=1,2,3$ for the north, east and vertical component) are modelled by the following relation:

$$y_k(t) = A_k + v_k t + B_{2k} \sin 2\pi t + B_{2k} \cos 2\pi t + \sum_{i=1}^n g_{ki} H(t - T_i) + \epsilon_k(t)$$

where A_k and v_k are respectively the intercept and constant rate. B_k ($B_k = \sqrt{B_{2k}^2 + B_{2k}^2}$) is the amplitude of the annual periodic signal. The g_{ki} terms are the offset magnitudes for the N identified discontinuities due to instrumental changes or seismic events eventually occurred at the T_i epochs. H is the Heaviside step function, and $\epsilon_k(t)$ are the measurement errors, that can be considered time correlated.

European reference frame

Figure 4. We have combined our solution (Northern - Central Italian network) with the results of other regional European networks (EUREF, REGAL, AMON) in the International Terrestrial Reference Frame (ITRF2005). Figure 4a shows the residual horizontal kinematic pattern with respect to a fixed Eurasian frame realized by minimizing the rigid motion of the EUREF stations located in the stable Central Europe, (Euler pole at 55.330°N, 95.979°W, $\omega = 0.2617$ "/Myr, Altamimi et al., 2007). In order to investigate which is the real geophysical significance of the computed vertical velocities (Figure 4b) of the GPS sites located in the Italian region, it can be noted that the global vertical velocities field obtained in this Reference Frame is in good agreement with the vertical displacements measured by the tide gauges network, and shows also an overall agreement with the Glacial Isostatic Adjustment (GIA), this process could affect the Europe south of Fennoscandia, inducing a prevalent uplift north of the 48th parallel. The small subsiding areas shown in figure and located almost above the 48th parallel of latitude, are generally inferred by one or few velocity data that do not seem to be consistent with nearby stations, and may be connected with regional and local tectonic structures (LODZ and CATO stations, Mid Polish Trough and its sedimentary infill) and oil/gas production (GWWL station, western Poland).

Acknowledgments

We are grateful to the following Institutions: ASI, ARPA Piemonte, FOGER (Fondazione dei Geometri e Geometri Laureati dell'Emilia Romagna), FREDNET (OGS), IREALP-Regione Lombardia, LABTOPO (University of Perugia), LEICA-Italtop, Regione Abruzzo, Regione Liguria, Regione Friuli Venezia Giulia, Regione Veneto, Regione Piemonte, RING-INGV, Provincia di Bolzano, Provincia di Trento, STONEX, which have kindly made available GPS recordings. This research was financially supported by the Ministry of Research (MIUR) and the National Space Agency (ASI). We are very grateful to Settore - Coordinamento Regionale Prevenzione Sismica Dir. Gen. Politiche Territoriali e Ambientali Regione Toscana and Servizio Geologico, Sismico e dei Suoli Regione Emilia Romagna for the economic and logistic support.

References

Altamimi, Z., Collilieux, X., Legrand, J., Garayt, B., Boucher, C., 2007. ITRF2005: a new release of the International Terrestrial Reference Frame based on time series of station positions and Earth Orientation Parameters. *J. Geophys. Res.* 112, B09401. doi:10.1029/2007JB004949.

Baldi, P., Casula, G., Cenni, N., Laddo, F., Pesci, A., 2009. GPS-based monitoring of land subsidence in the Po Plain (Northern Italy). *Earth Planet. Science Lett.* 288, 204-212. doi:10.1016/j.epsl.2009.09.023.

Cenni, N., Casula, G., Cenni, N., Laddo, F., Pesci, A., and Bacchetti, M., 2011. Vertical axial crustal movements in Central and Northern Italy. *Bull. Soc. Geol. It.* (Ital. J. Geosci.), 52, n.4, pp. 667-685.

Cenni, N., Mantovani, E., Baldi, P., Viti, M., 2012. Present kinematics of Central and Northern Italy from continuous GPS measurements. *J. Geodyn.* 58, pp. 62 - 72. doi:10.1016/j.jog.2012.02.004.

Finetti, I.R., Boccalini, M., Bonini, M., Del Ben, A., Pipan, M., Prizon, A., Sani, F., 2005. Lithospheric Tectono-Stratigraphic Setting of the Ligurian Sea-Northern Apennines-Adriatic Foreland from Integrated CROP Seismic Data. In: Finetti, I.R. (Ed.), *Deep Seismic Exploration of the Central Mediterranean and Italy*. CROP PROCEEDINGS. Elsevier, Amsterdam, pp. 119-158.

Funicello, R., Paretto, M., Prati, A., Bigi, G. (Coord.), 1981. Carta Tettonica d'Italia alla scala 1:1500000. CNR Progetto Finalizzato Geodinamica. Pubbl. 269. Grafica Editoriale Cartografica, Roma.

Mantovani, E., Babbucci, D., Tamburelli, C., Viti, M., 2009a. A review on the driving mechanism of the Tyrrhenian-Apennines system: Implications for the present seismotectonic setting in the Central-Northern Apennines. *Tectonophysics* 476, 22-40. doi:10.1016/j.tecto.2008.10.032.

Mantovani, E., Viti, M., Babbucci, D., Ferrini, M., D'Introna, V., Cenni, N., 2009b. Quaternary geodynamics of the Apennine belt. *Il Quaternario* 22, 97-108.

Viti, M., Mantovani, E., Babbucci, D., Tamburelli, C., 2006. Quaternary geodynamics and deformation pattern in the Southern Apennines: implications for seismic activity. *Bull. Soc. Geol. It.* 125, 273-291.

Viti, M., Mantovani, E., Babbucci, D., Tamburelli, C., 2011. Plate kinematics and geodynamics in the Central Mediterranean. *Tectonophysics* 51, 190-204. doi:10.1016/j.tecto.2010.02.008.

Emilia earthquakes: first results

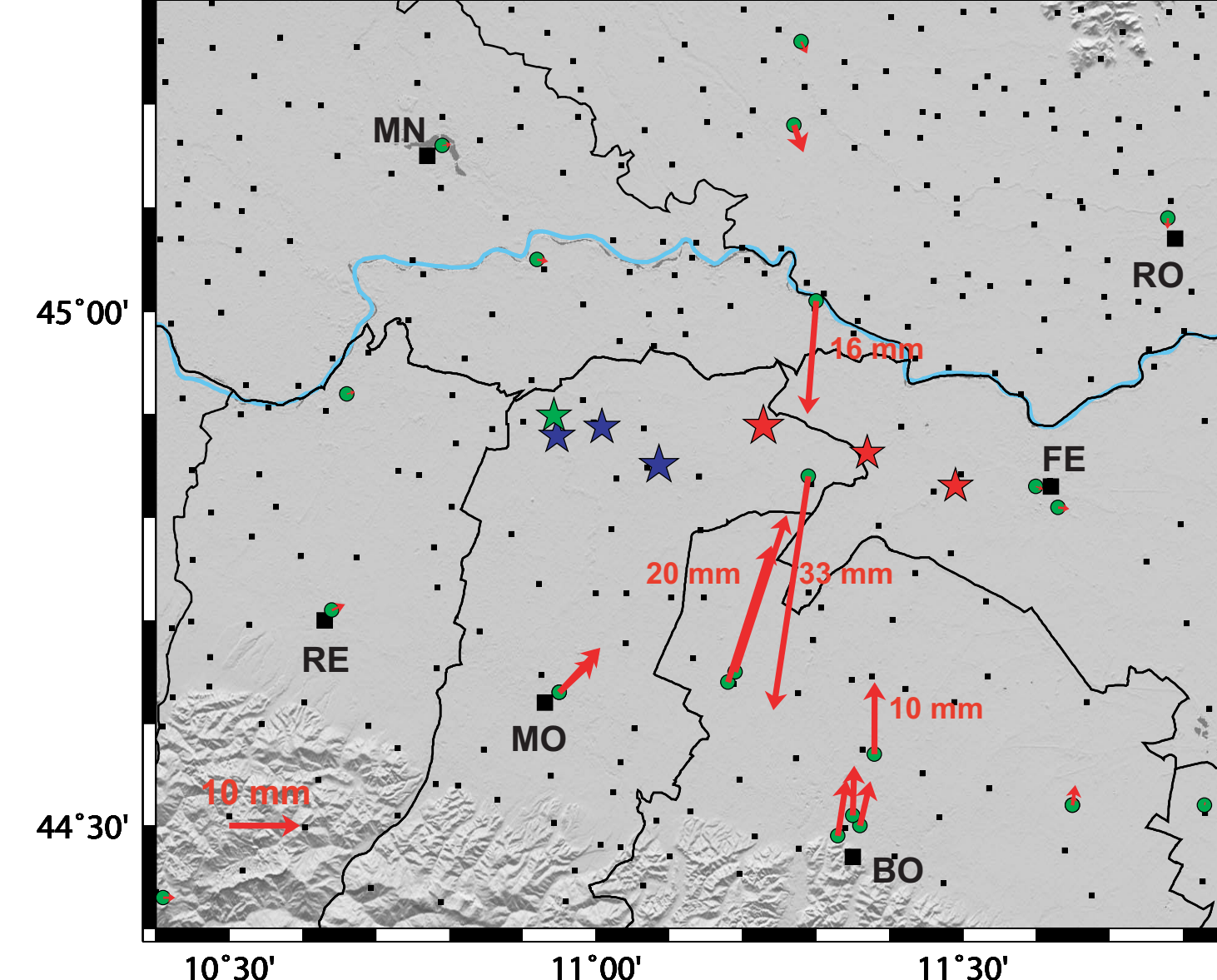


Figure 8. GPS coseismic horizontal displacements for the 20 May seismic events. The red and blue stars respectively show the position of the May 20 and 29 principal events ($M > 5$). The green star indicates the position of the June 3 earthquake.

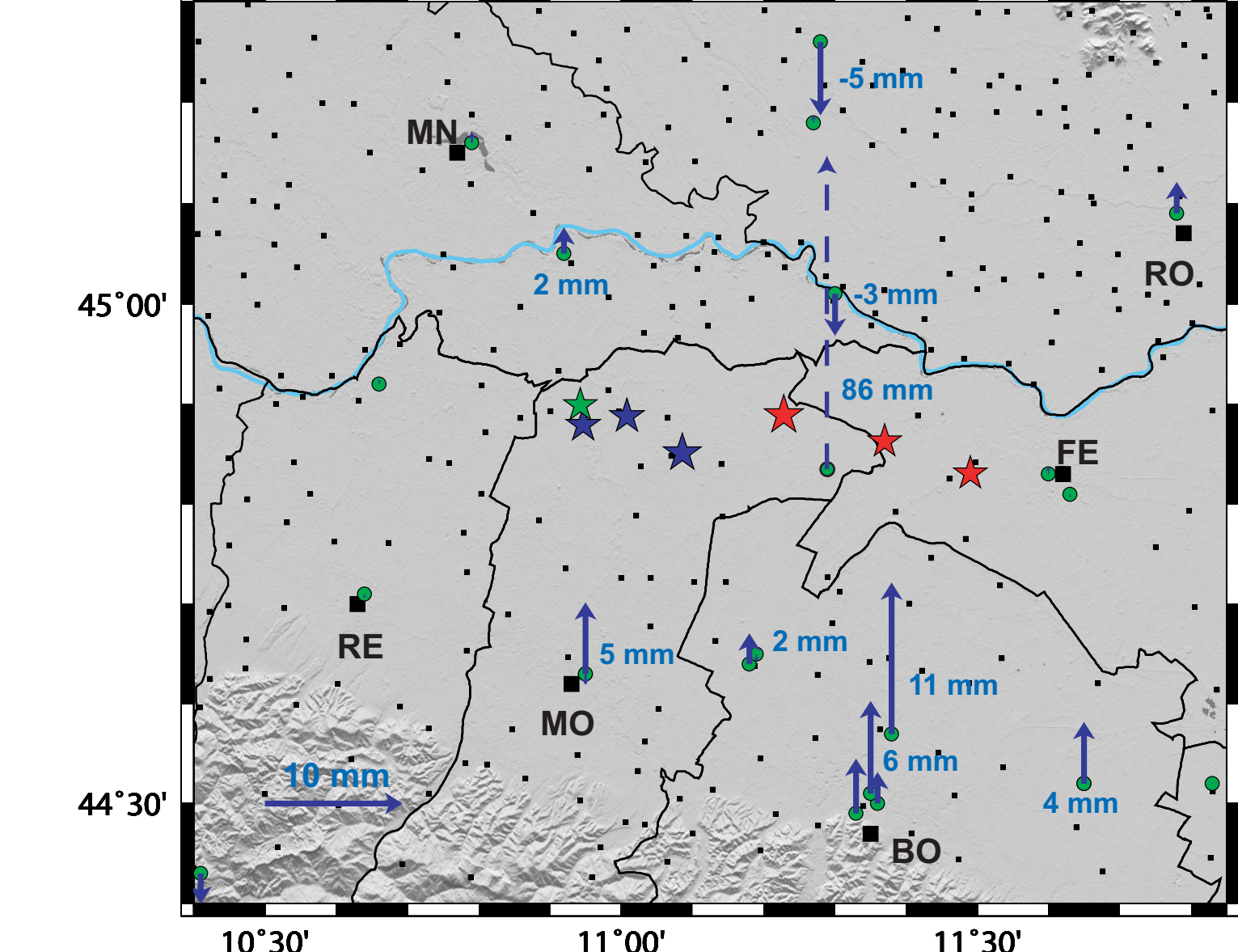


Figure 9. First estimation of the vertical coseismic displacement for the GPS sites located near the May 20 earthquake and aftershocks (red stars).

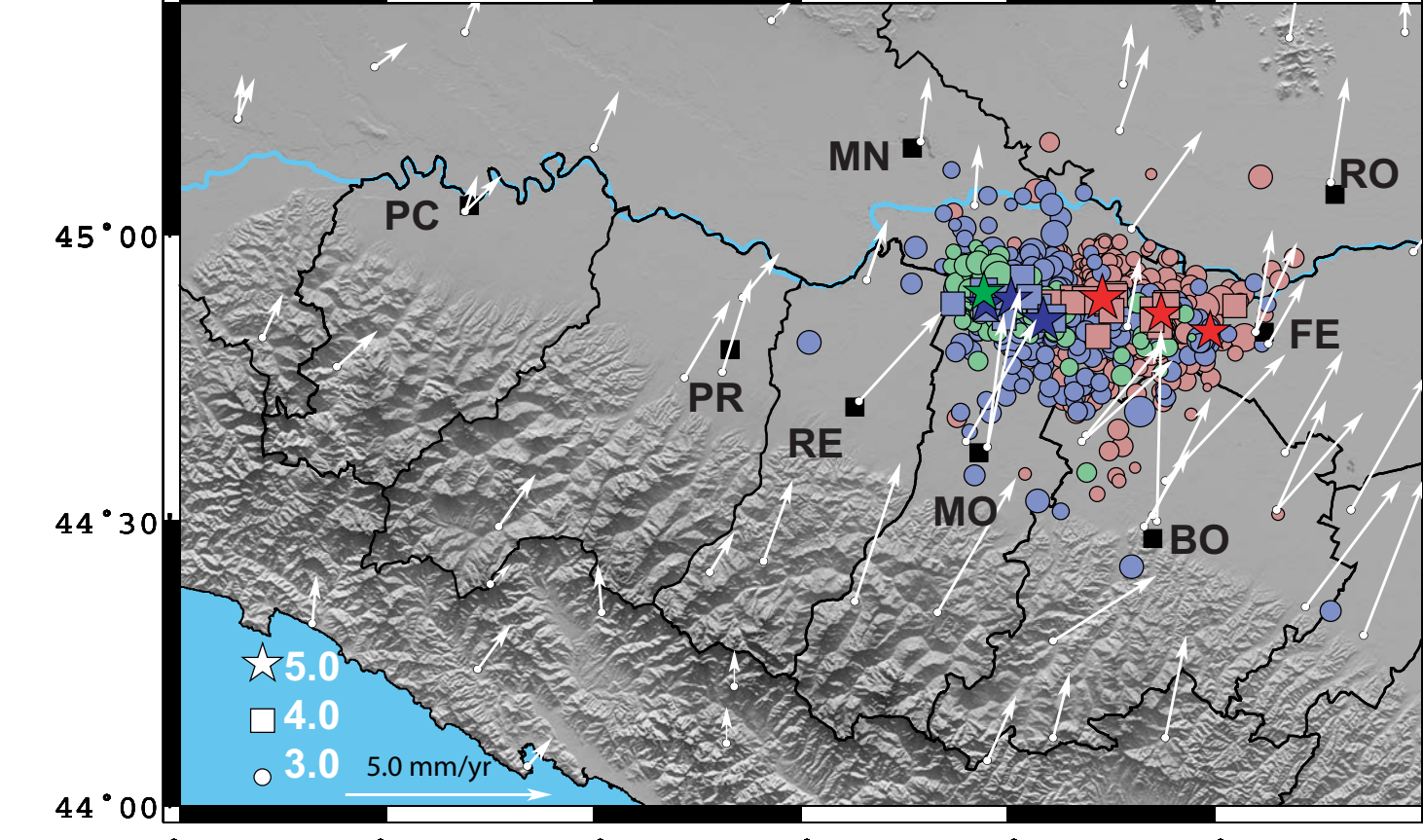


Figure 10. Red, blue and green circles, squares and stars respectively represent the epicenters of events with $1 < M < 4$, $4 < M < 5$ and $M > 5$ overlapped to a particular of the GPS velocity field shown in Fig. 5a.

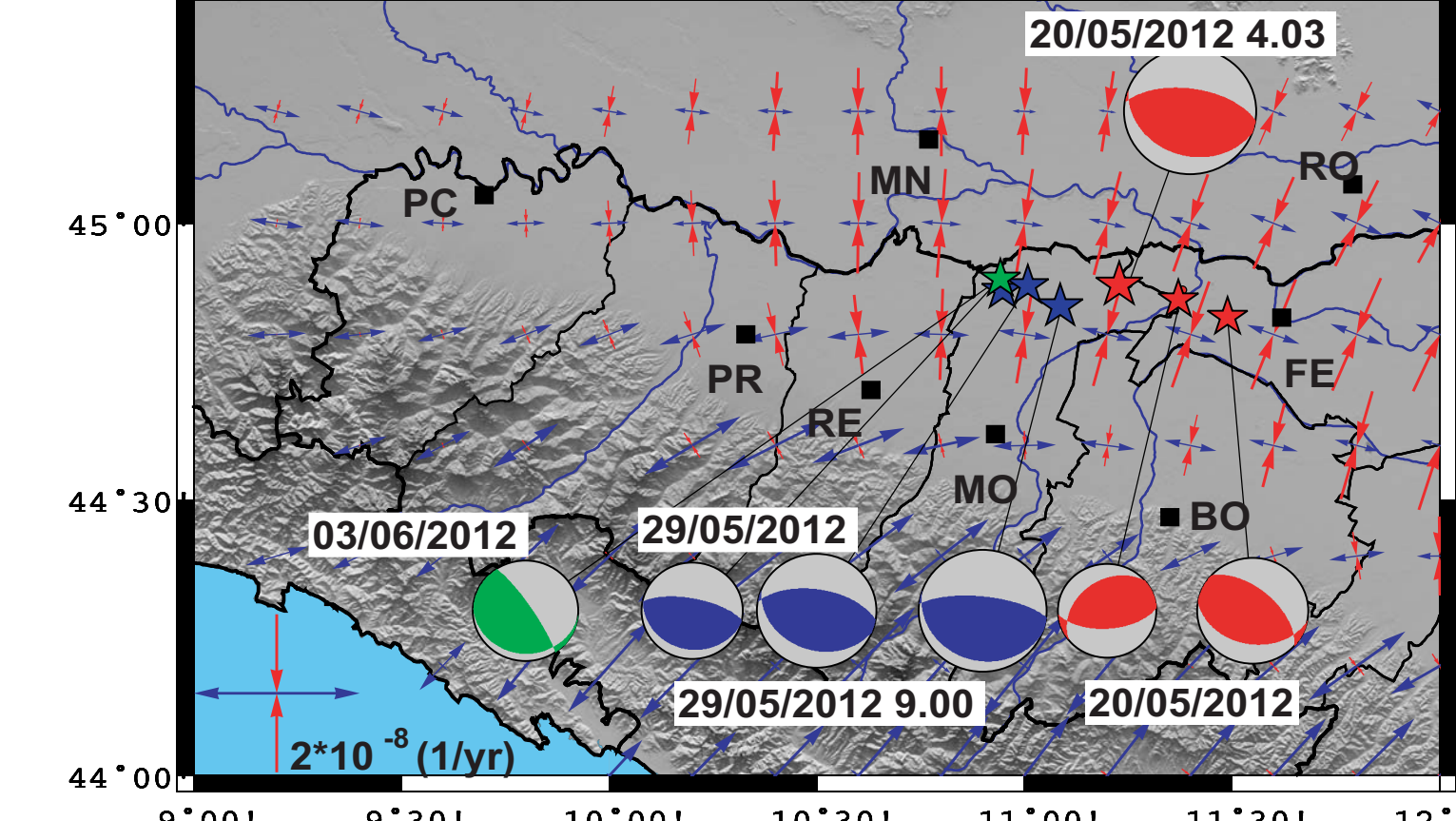


Figure 11. Main events (stars) and respective focal mechanisms of the Emilia seismic sequence. It is worth noting that the shortening axes deduced from focal mechanisms are quite compatible with the strain field resulting from GPS data (Fig. 5c).